Journal of Physics: Conference Series **131** (2008) 012028 doi:10.1088/1742-6596/131/1/012028

High Spatial Resolution Observations of the T Tau System – I. Astrometry in the near-infrared

Rainer Köhler

ZAH, Landessternwarte, Königstuhl, 69117 Heidelberg, Germany

E-mail: rkoehler@lsw.uni-heidelberg.de

Abstract. T Tauri is an example how our knowledge about an object improves with spatial resolution: About 60 years ago, it was considered to be the prototypical T Tauri star. 25 years ago, it was discovered to be a close binary with an infrared companion at 0.7 arcsec distance. Ten years ago, the infrared companion was itself resolved into a binary with just 50 mas separation. We collected astrometric data from the literature and from archived VLT observations. Additionally, we present a new measurement obtained on February 1, 2008. Fits of orbit models to the data yield estimates for the orbital elements of the close binary. In most other binaries, we can observe only the relative motion of both components around each other, which can be used to determine the total mass of the pair. The presence of the third component in the T Tauri system gives us the rare opportunity to observe also the motion of both components of the close binary around their common center of mass, allowing to determine dynamical masses of the individual stars. We find that the period of the best model for the orbit of T Tau Sa and Sb is 28^{+12}_{-4} years. The mass of Sa is $2.28 \pm 0.22\,\mathrm{M}_\odot$ and the mass of Sb is $0.41 \pm 0.19\,\mathrm{M}_\odot$.

1. A short history of T Tauri

T Tauri was discovered in 1852 by Hind during observations of the bright variable nebula NGC 1555 (Hind's nebula) [1]. Almost a century later, Joy defined a new class of variables and named them "T Tauri variables" [2], because T Tau not only shows the typical features, but also is among the brightest and best known objects of this group. Ambartsumiam suggested that these stars are low-mass pre-main-sequence objects [3].

Dyck et al. observed T Tau using one-dimensional speckle interferometry and found an infrared companion with a separation of less than one arcsecond [4]. This southern component dominates the system longward of the near-infared wavelength regime, but no optical counterpart could be identified down to 19.6 mag in the V-band [5].

Considerable observational and theoretical effort has been expended to understand this source. Again, higher spatial resolution provided an important clue for solving this puzzle: Koresko resolved the southern companion into two sources using speckle holography at the Keck telescope [6]. With a separation of $\sim 0.05''$, the two components were named T Tau Sa and T Tau Sb. T Tau Sb has been identified as a heavily extincted, actively accreting pre-main-sequence star with a spectral type M1 [7], while the spectrum of T Tau Sa is featureless except for a strong Brγ emission line, leaving the nature of the object uncertain.

The northern of the two radio sources found by Schwartz et al. [8] is easy to identify with T Tau N, but it was not clear which of the two components of T Tau S should be identified

with the southern radio source. Johnston et al. and Loinard et al. associated the radio source with T Tau Sb [9, 10, 11]. This would require that the orbital motion of T Tau Sb around T Tau Sa shows a dramatic change between 1995 and 1998, probably caused by the ejection of Sb from the T Tau S system [10]. However, Furlan et al. found that T Tau Sb and the radio source have distinct paths, and suggested a fourth object as the source of the southern radio emission [12]. On the other hand, Johnston et al. [13, 14] presented an orbital fit to the IR and radio data simultaneously. The residuals between the orbit model and the IR data are of the order of the measurement errors, while the residuals of the radio data exceed the accuracy of the measurements. The authors concluded that the radio source may be connected with, but not identical to the infrared source.

The presence of the companion Sb at such a small separation offers the possibility to trace the orbital motion of T Tau Sa and Sb around each other in a reasonable time and with no influence of T Tau N in first order approximation. This allows us to determine the dynamical mass of T Tau S. With the help of the common orbit of the southern pair around the northern component, we can also determine the individual masses of T Tau Sa and Sb.

Such an analysis has been carried out by Duchêne et al. and Köhler et al. [15, 16]. The main difference between both studies is that Duchêne et al. combined radio and infrared observations to increase the coverage of the orbit, while Köhler et al. used only observations in the near infrared to ensure that the positions of the stars themselves are measured. In this work, we present an update on our ongoing monitoring program of the T Tauri system.

2. Observations

We used all the astrometric measurements of the T Tau system listed in Köhler et al. [16], both collected from the literature and from our own observations with NACO, the adaptive optics, near-infrared camera at the ESO Very Large Telescope on Cerro Paranal, Chile [17, 18]. These data were augmented by a new measurement obtained with NACO on February 1., 2008 (figure 1). Standard NIR-data reduction methods were applied to the images, i.e. a median sky image was subtracted, the images were divided by a flat field, and bad pixels were replaced by the median of the closest good neighbors. The positions of the stars were measured with the Starfinder program [19].

2.1. Astrometric Calibration

One important aspect of astrometric measurements is the determination of the exact pixel scale and detector orientation at the time of the observation. Since there are no reference stars in the field-of-view around T Tauri, we took images of a field in the Orion Trapezium cluster immediately after the images of T Tauri. The measured positions of stars in the Trapezium images were compared with the coordinates in McCaughrean and Stauffer [20] by the astrometric software ASTROM[1]. In the past, we neglected (relative) proper motions, since no proper motions for these stars have been published. The positions of the stars were measured in 1993, the unknown systematic error caused by this approach is growing with time.

We took images of the same region in the Orion Trapezium almost yearly since December 2002. This database can be used to estimate relative proper motions of the stars in our images. Since the proper motions and the pixel scale/orientation of the images depend on each other, we have to use an iterative procedure. To do this, we first determine the pixel scale and orientation of the images without taking proper motions into account. Then, the measured (pixel) positions of the stars are used to compute improved R.A. and Dec. at the epoch of the observations. Observations at different epochs (including the coordinates in [20]) are used to estimate the proper motions. With these estimates, we compute improved positions at the

[1] see http://www.starlink.rl.ac.uk/star/docs/sun5.htx/sun5.html

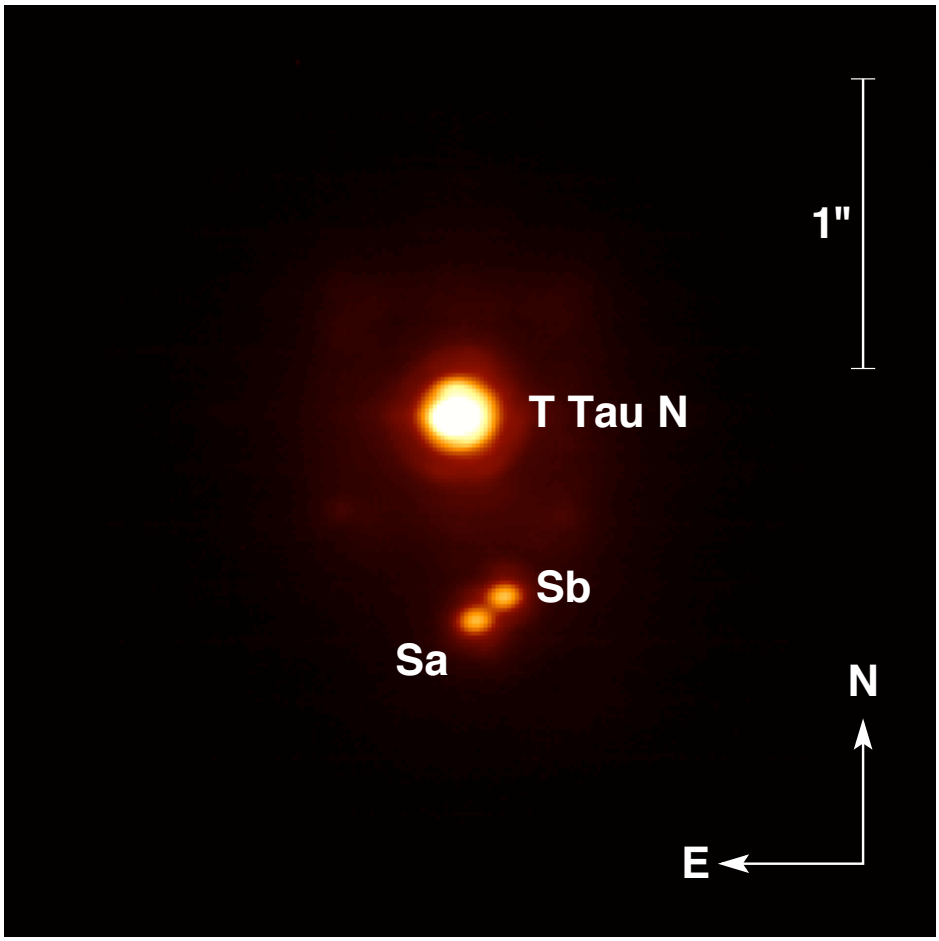

Figure 1. Image of the T Tau system taken with NACO in the K_s photometric band on 2008 February 1, shown with a logarithmic scale.

times of the observations, which in turn are used to compute better estimates for pixel scale and orientation. This procedure is repeated several times. In each step, the scatter of the pixel scale and orientation at one epoch is computed. This scatter decreases during the first iterations and levels off after about the eighth iteration. We take this as indication that our method actually improves the astrometric calibration.

The scatter of the pixel scale is very small, less than 1 % of the pixel scale itself (table 1). The scatter of the orientation is on the order of a few tenths of a degrees. This is what we would expect, since there is no reason why the pixel scale should change much, while the orientation depends on the precision and repeatability of the rotator of the VLT and inside NACO. The rotators have a precision of a few tenths of a degree (Wolfgang Brandner, priv. comm.), which explains our results.

The relative positions of the components of the T Tauri system derived with these calibrations appear in table 2. To account for changes in pixel scale and orientation between the observation of the Trapezium field and T Tau, a systematic error of 0.02 mas/pixel and 0.1° was added.

Table 1. Pixel Scale and Orientation of our Observations.

Epoch	Pixel scale [mas/pixel]	Position Angle of the y-axis [degrees]
Dec. 2002	13.232 ± 0.025	0.186 ± 0.241
Dec. 2003	13.248 ± 0.041	-0.199 ± 0.101
Dec. 2004	13.235 ± 0.003	-0.321 ± 0.022
Dec. 2006	13.221 ± 0.004	0.044 ± 0.013
Sep. 2007	13.231 ± 0.003	0.158 ± 0.035
Feb. 2008	13.231 ± 0.004	0.151 ± 0.021

Table 2. Relative Positions in the T Tauri System on February 1., 2008

	Separation [mas]	Position Angle [degrees]
N-Sa	692.4 ± 1.1	185.63 ± 0.10
N-Sb	628.6 ± 2.4	195.14 ± 0.10
Sa-Sb	126.59 ± 0.23	310.53 ± 0.14

3. Orbit Determination

3.1. The orbit of T Tau Sa/Sb

To determine the orbital elements of the binary Sa/Sb, we follow the method described in [16]. The procedure consists of two steps: First, a grid search in Period P, eccentricity e and time of periastron T_0 is carried out, while Singular Value Decomposition is used to solve the linear equation system for the four Thiele-Innes constants. From the Thiele-Innes constants, the remaining orbital elements (semi-major axis a, argument of periastron ω, position angle of the line of nodesΩ , and inclination i) are computed. The result of the grid search is χ^2 as function of P and e, which helps to assess the quality of the fit, and the confidence limits of the fit parameters.

In the second step, all 7 orbital elements are fit simultaneously using a Levenberg-Marquardt algorithm. This improves the fit further by interpolating between grid points and ensures that all 7 elements are treated equally in the final fit. To avoid that the algorithm converges on a local instead of the global minimum, we decided to use *all* orbits resulting from the grid-search as starting points and carried out 250×200 runs of the Levenberg-Marquardt algorithm (the grid spans 250 periods and 200 eccentricities).

The orbit with the globally minimum χ^2 appears in table 3 and figure 2. Compared to our results in [16], we now find a shorter period (93 years previously, now 28 years). This is mostly caused by the latest data point from February 2008, which demonstrates how every new data point contributes to our knowledge of the orbit. The new orbit with the shorter period is in better agreement with the results of orbit fits to both IR and radio data [13, 15].

3.2. The orbit of T Tau N/S

The positions of T Tau Sb relative to Sa allow us to determine only the combined mass of Sa and Sb. To compute the individual masses, we need to know the mass ratio q, which can be

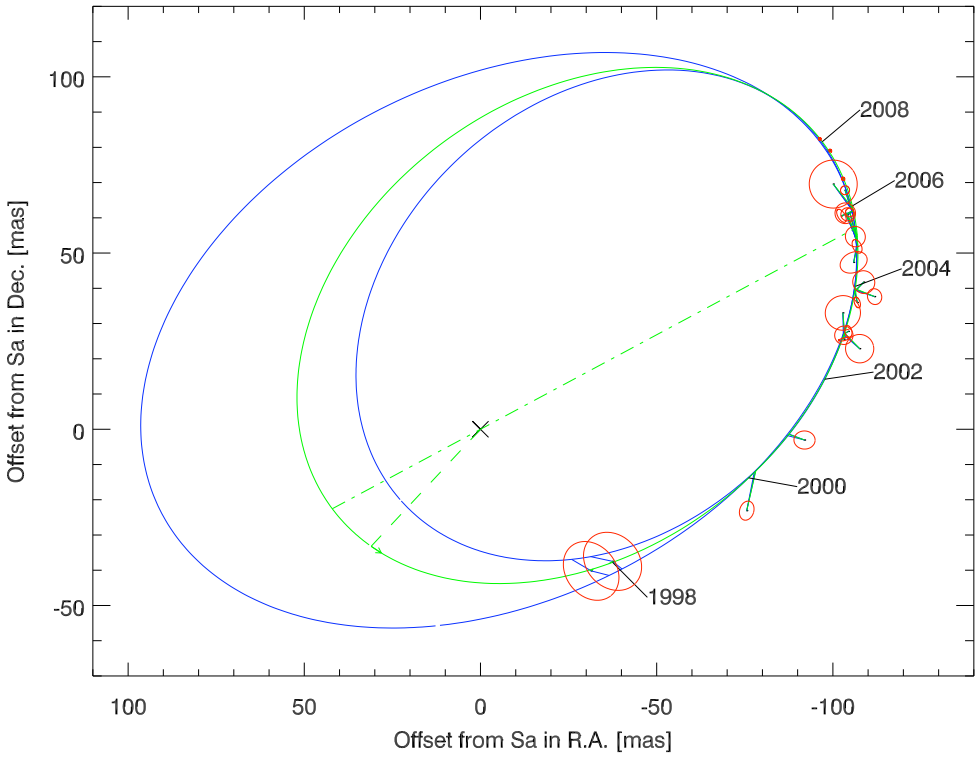

Figure 2. Results of our orbit fits for the Sa/Sb pair. The measurements are indicated by the red ellipses, the best orbit model is shown in green. The dashed line marks the periastron, the dash-dotted line the line of nodes. Two orbits at the 90 % confidence limit for the period are shown in blue, their periods are 24 and 40 years. The positions on the first of January in the years 1998 to 2008 are marked.

computed if the position of the center of mass (CM) of Sa and Sb is known. Unfortunately, we cannot observe the CM directly. However, we know that the CM of Sa and Sb is in orbit around T Tau N, and that Sa and Sb are in orbit around their CM. The CM is always on the line between Sa and Sb, and its distance from Sa is the constant fraction $q/(1+q)$ of the separation of Sa and Sb. The positions of Sa and Sb are usually observed at the same time as N, so we can use the *observed* separation vectors Sa-Sb to constrain the position of the CM.

Our model describes the position of the CM of Sa and Sb in two ways: First, it is on a Keplerian orbit around N, which is described by 7 orbital elements. Second, the position of the CM can be computed from the positions of Sa and Sb, and the mass ratio (which is treated as a free parameter). Standard error propagation is used to obtain an error estimate for this position. To compute χ^2, we compare the position of the CM from the orbit around N with the positions derived from the observations. See [16] for a more detailed explanation.

The fitting procedure is similar to that used for the orbit of Sa/b, except that the grid-search is carried out in 4 dimensions: eccentricity e, period P, time of periastron T_0, and the fractional mass f. Singular Value Decomposition was used to fit the Thiele-Innes constants, which give

Table 3. Parameters of the best orbital solutions for the Sa–Sb and the N–S binary.

Orbital Element	Orbit Sa–Sb	Orbit N–S
Date of periastron T_0	$2449882\,^{+350}_{-300}$	$2453985\,^{+8500}_{-1000}$
	(1995 Jun 13)	(2006 Sep 6)
Period P (years)	$28\,^{+12}_{-4}$	$17535\,^{+7500}_{-16000}$
Semi-major axis a (mas)	$87\,^{+39}_{-12}$	$8392\,^{+8000}_{-4000}$
Semi-major axis a (AU)	$13\,^{+6}_{-2}$	$1231\,^{+1174}_{-587}$
Eccentricity e	$0.47\,^{+0.16}_{-0.18}$	$0.92\,^{+0.07}_{-0.08}$
Argument of periastron ω (°)	$22.4\,^{+84.0}_{-56.0}$	$191.3\,^{+9.0}_{-3.0}$
P.A. of ascending node Ω(°)	$118.2\,^{+66.0}_{-6.0}$	$360.0\,^{+12.0}_{-3.0}$
Inclination i (°)	$34.8\,^{+12.0}_{-31.0}$	$56.1\,^{+3.0}_{-4.0}$
System mass M_S ($M_\odot$)	$2.70\,^{+0.12}_{-0.05}$	$6.07\,^{+0.07}_{-0.54}$
reduced χ^2	3.9	4.3
Mass ratio $M_{\rm Sb}/M_{\rm Sa}$	0.18 ± 0.10	
Mass of Sa $M_{\rm Sa}$ ($M_\odot$)	$2.28\,^{+0.22}_{-0.20}$	
Mass of Sb $M_{\rm Sb}$ ($M_\odot$)	$0.41\,^{+0.19}_{-0.19}$	

the remaining orbital elements. The grid-point with the smallest χ^2 was used as starting point for a Levenberg-Marquardt fit. Since this fit method assumes that the measurement errors are independent of the fitting parameters, q cannot be treated like the other parameters. Instead, we perform a grid search over a narrow range in q to find the minimum.

Fits to small sections of an orbit often result in unphysically high system masses (several $100\,\mathrm{M}_\odot$). Such an orbit is clearly not a good solution, even if its χ^2 is very small. To prevent the Levenberg-Marquardt fit from exploring unphysical regions of parameter space, we added a mass constraint to the computation of χ^2. We expect the total system mass of T Tau N, Sa, and Sb to be $4.7 \pm 1\,\mathrm{M}_\odot$. This is a reasonable estimate based on our results in Sect. 3.1 for the total mass of T Tau S and the mass of T Tau N derived from its spectral energy distribution [21].

An important question is whether we want to include observations that did not resolve T Tauri S in the fit. These measurements yield only the position of the center of *light* of Sa/b, not the center of *mass*. The offset between the two centers is unknown and not even constant, since both components are photometrically variable [22]. On the other hand, the data obtained before the binary nature of T Tauri S was discovered almost double the fraction of the orbit that has been observed so far.

To answer this question, we tried both ways. The left panel of figure 3 shows the result of the fit if we exclude observations that did not resolve Sa/Sb. The best-fitting model orbit deviates significantly from positions measured before 1995. Furthermore, the mass ratio this fit yields is 0.88, which gives a mass of $1.26\,\mathrm{M}_\odot$ for Sb. This is not compatible with its spectral type of about M1.

The right panel of figure 3 shows the resulting orbit if all observations are used, under the assumption that unresolved observations measured the position of the center of mass. This orbit fits all measurements rather well. The mass ratio Sb:Sa is 0.18, i.e. we obtain a mass of Sa of

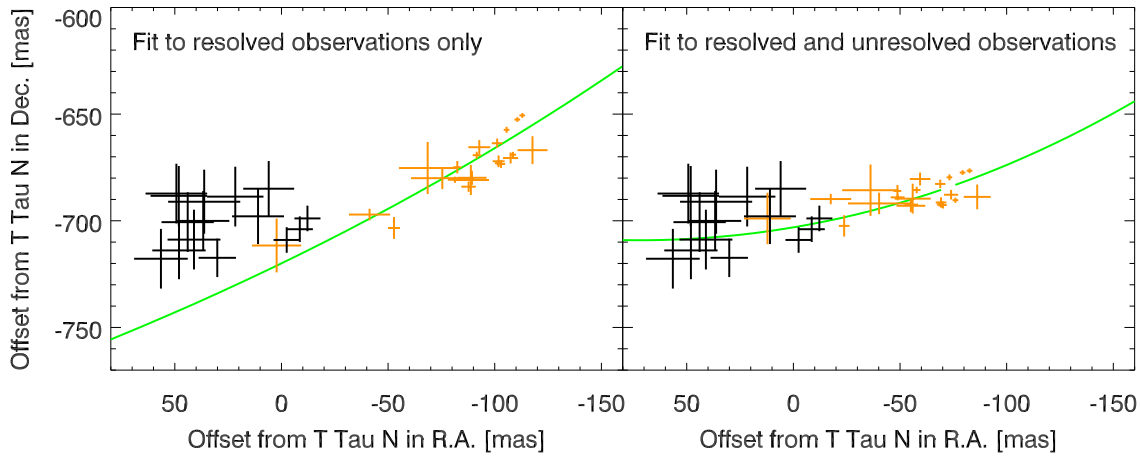

Figure 3. Results of our orbit fits for the N/S binary. Measurements that did not resolve the Sa/Sb-pair are indicated by the black crosses, measurements that did resolve the tight pair are orange. Note that in the latter case, the position of the center of mass is shown, which depends on the model parameter q. Since the mass ratio q in the two models is different, the center of mass in the resolved observations shifts between the two cases. The green line marks the best-fitting orbit. The left panel shows the results if we use only observations that did resolve Sa and Sb (i.e. the orange crosses). The right panel shows the results if we include observations that did not resolve Sa/Sb and assume that the measured position is identical with the center of mass of the southern binary.

$2.28 \pm 0.22\,M_\odot$, while the mass of Sb is $0.41 \pm 0.23\,M_\odot$, in agreement with its spectral type of early M. The total mass of the system resulting from the fit is about $6\,M_\odot$, somewhat larger than our best guess of $4.7\,M_\odot$. We take this as sign that, although our orbit is the best model with the data at hand, the true orbit might be quite different.

4. Conclusions and Outlook

We have collected all available near-infrared astrometric data on the T Tauri system from the literature. We also present a new data point obtained with NACO at the VLT on February 1, 2008. Binary orbit models were fitted to the relative positions of T Tau Sa and Sb in order to estimate the orbital elements. We find that most elements are not very well constrained, e.g. the period is 28^{+12}_{-6} years. This period is significantly shorter than found by [16], mainly due to the data point from February 2008. This demonstrates that the orbit is still not well constrained, and that every new measurement brings an important contribution to the orbit determination.

The shorter period is in better agreement with orbit determinations based on IR- and radio data [13, 15]. This indicates that the radio source is related to T Tauri Sb, although the exact nature of this relation remains unclear.

The total mass of the T Tau S binary can be estimated to be $2.7^{+0.12}_{-0.05}\,M_\odot$, which is only 10 % smaller than the previous mass estimate [16]. The orbit of T Tau N and T Tau S around each other has probably a period of several thousand years. Because of the very small fraction of the orbit that has been observed so far, the orbital parameters are only poorly constrained. However, the orbital motion of T Tau S around N allows to estimate the positions of the center of mass of T Tau S, which gives an estimate for the mass ratio Sa:Sb. We obtain masses of

2.28 ± 0.22 and $0.41 \pm 0.19\,M_\odot$ for Sa and Sb, resp. Therefore, the infrared companion Sa is probably the most massive component.

We will continue to monitor the system astrometrically, in order to get closer to understanding this surprisingly mysterious system.

Acknowledgments
I wish to thank my colleagues T. Ratzka, T. M. Herbst, M. Kasper, E. Meyer, and M. Stumpf for contributions to and helpful discussions about this project.

References

[1] Hind J R 1864 *MNRAS* **24** 65–65
[2] Joy A H 1945 *ApJ* **102** 168–199
[3] Ambartsumian V A 1947 *Stellar Evolution and Astrophysics* (Yerevan: Acad. Sci. Armenian SSR)
[4] Dyck H M, Simon T and Zuckerman B 1982 *ApJ* **255** L103–L106
[5] Stapelfeldt K R, Burrows C J, Krist J E, Watson A M, Ballester G E, Clarke J T, Crisp D, Evans R W, Gallagher John S I, Griffiths R E, Hester J J, Hoessel J G, Holtzman J A, Mould J R, Scowen P A, Trauger J T and Westphal J A 1998 *ApJ* **508** 736–743
[6] Koresko C D 2000 *ApJ* **531** L147–L149
[7] Duchêne G, Ghez A M and McCabe C 2002 *ApJ* **568** 771–778
[8] Schwartz P R, Simon T, Zuckerman B and Howell R R 1984 *ApJ* **280** L23–L26
[9] Johnston K J, Gaume R A, Fey A L, de Vegt C and Claussen M J 2003 *AJ* **125** 858–867
[10] Loinard L, Rodríguez L F and Rodríguez M I 2003 *ApJ* **587** L47–L50
[11] Loinard L, Mioduszewski A J, Rodríguez L F, González R A, Rodríguez M I and Torres R M 2005 *ApJ* **619** L179–L182
[12] Furlan E, Forrest W J, Watson D M, Uchida K I, Brandl B R, Keller L D and Herter T L 2003 *ApJ* **596** L87–L90
[13] Johnston K J, Fey A L, Gaume R A, Claussen M J and Hummel C A 2004 *AJ* **128** 822–828
[14] Johnston K J, Fey A L, Gaume R A, Hummel C A, Garrington S, Muxlow T and Thomasson P 2004 *ApJ* **604** L65–L68
[15] Duchêne G, Beust H, Adjali F, Konopacky Q M and Ghez A M 2006 *A&A* **457** L9–L12
[16] Köhler R, Ratzka T, Herbst T M and Kasper M 2008 *A&A* **482** 929
[17] Rousset G, Lacombe F, Puget P, Hubin N N, Gendron E, Fusco T, Arsenault R, Charton J, Feautrier P, Gigan P, Kern P Y, Lagrange A M, Madec P Y, Mouillet D, Rabaud D, Rabou P, Stadler E and Zins G 2003 *Adaptive Optical System Technologies II* (*SPIE Proceedings* no 4839) ed Wizinowich P L and Bonaccini D pp 140–149
[18] Lenzen R, Hartung M, Brandner W, Finger G, Hubin N N, Lacombe F, Lagrange A M, Lehnert M D, Moorwood A F M and Mouillet D 2003 *Instrument Design and Performance for Optical/Infrared Ground-based Telescopes* (*SPIE Proceedings* no 4841) ed Iye M and Moorwood A F M pp 944–952
[19] Diolaiti E, Bendinelli O, Bonaccini D, Close L, Currie D and Parmeggiani G 2000 *A&AS* **147** 335–346
[20] McCaughrean M J and Stauffer J R 1994 *AJ* **108** 1382
[21] Loinard L, Torres R M, Mioduszewski A J, Rodríguez L F, González-Lópezlira R A, Lachaume R, Vázquez V and González E 2007 *ApJ* **671** 546–554
[22] Beck T L, Schaefer G H, Simon M, Prato L, Stoesz J A and Howell R R 2004 *ApJ* **614** 235–251